International Conference on Applied Energy 2021
Nov. 29 - Dec. 2, 2021, in Bangkok, Thailand
Paper ID: 144

Cycle Power and Efficiency Modelling of Stirling Engines based on Modified Second-order Adiabatic Analysis and Improved Atom Search Integrated Back-propagation Neural Network

Jiying Chen[1], Rui Zhao[1], Kai H. Luo [1*]

1 Department of Mechanical Engineering, University College London, Torrington Place, London WC1E 7JE, United Kingdom

ABSTRACT

The broad adaptability of the Stirling engine to a variety of heat sources makes it a promising technology for industrial waste heat recovery. The operation of the Stirling engine involves a multi-physics coupled process of heat transfer and fluid mechanics as well as non-linear losses due to mechanical friction and gas charge leaking. Therefore, accurate modelling of Stirling engine power output through theoretical analysis is complex and costly. In this study, a modified second-order adiabatic model is developed, and the Runge-Kutta method is introduced to obtain numerical solutions. Furthermore, to determine the fuzzy mapping relationship between the numerical results and the actual experiments and consider the power output and operation efficiency simultaneously, a back-propagation neural network with two neurons in the output layer that is used to export the power and corresponding efficiency is established. To accomplish the optimum performance, a novel improved atom search optimisation algorithm (IASO) retooled by elite opposition-based learning and dimensional Gaussian mutation is proposed to optimise weights and thresholds of neural networks selected. Results of the IASO-BP integrated model indicate that the simultaneous modelling of power and efficiency can obtain 95% accuracy on the Stirling engine under study. Finally, to achieve a close integration between research and industry, a regional microgrid containing Stirling engines and rooftop photovoltaic panels for supercomputers waste heat recovery is designed. Multi-objective optimisation for energy systems is implemented and deep complementarity between energy supply and loads is finally achieved.

Keywords: Waste Heat Recovery, Stirling Engine, Second-order Adiabatic Analysis, Back-propagation Neural Networks, Improved Atom Search Optimisation

NONMENCLATURE

Abbreviations	
ANN	Artificial Neural Network
ASO	Atom Search Optimization
BP	Back-Propagation
CAFS	Combined Adiabatic-Finite Speed
IASO	Improved Atom Search Optimization
ISAM	Improved Simple Analysis Model
PSML	Polytropic Model with Losses
Symbols	
c	Compression Chamber
k	Cooler
r	Regenerator
h	Heater
e	Expansion Chamber
V_{sp}	Swept Volume
V_{cl}	Clearance Volume
c_p	Heat Capacity at Constant Pressure
c_v	Heat Capacity at Constant Volume
Re	Reynolds Number
Pr	Prandtl number
ε	Efficiency of the Regenerator
$Q_{shuttle}$	Heat Losses due to Shuttle Movement
Q_{poly}	Polytropic Heat loss
Q_{reg}	Regenerator Losses

Selection and peer-review under responsibility of the scientific committee of the 13th Int. Conf. on Applied Energy (ICAE2021).

INTRODUCTION

Nowadays, the global energy sustainability and climate change are becoming increasingly serious issues. Clean energy and industrial waste heat recovery technologies have received growing attention worldwide. The Stirling engine has become an important technology due to its characteristics of versatility and operation stability. The Stirling engine works by the trapped gas absorbing the internal energy of heat sources, expanding thermally and producing mechanical work. As long as there is a temperature difference, the Stirling engine has the ability to produce work. Stirling engines are also environmentally friendly as there is no fuel combustion during operation [1]. However, a significant problem with the Stirling engine is that there are almost no satisfactory models for operation analysis [2]. This is because the working of a Stirling engine involves a variety of thermodynamically and mechanically coupled processes and is accompanied by several flow and heat transfer losses, all of which pose significant difficulties for classical mathematical modelling approaches. Researchers have made many attempts to model the Stirling engine. Cheng et al. [3] developed a non-isothermal model which considered the effects of non-isothermal processes, incomplete heat recovery and thermal resistance. They applied this to a 300 W Beta Stirling engine and found that the simulated shaft power values were approximately 12% to 20% higher than the experimental data. Timoumi and Tlili et al. [4] simulated the operation of a GPU-3 Stirling engine considering heat losses and pressure drop, and the prediction error of their proposed model was less than 10%. Ni et al. [5] developed an Improved Simple Analysis Model (ISAM) based on the ideal adiabatic model, taking into account the heat return losses and flow resistance losses. Li et al. [6] [7] developed a calculation scheme called Polytropic Model with Losses (PSML) and found that the non-ideal heat return losses and leakage losses of the heat exchanger were the main forms of energy dissipation.

Numerical methods considering multiple losses are getting closer to real operation, but there seems to be an accuracy threshold due to the numerical model itself. Considering the diminishing marginal cost effect, there may be little to gain by simply increasing the investment in numerical calculations. Combining numerical simulation results with the emerging field of deep learning would be a more promising approach. In section 2, several modifications to the classical adiabatic model are first implemented. Afterwards, a back-propagation neural network that contains the results of the numerical model and can export both output power and efficiency is constructed. Simultaneously, a novel improved atom search optimisation algorithm (IASO) is proposed to optimise the selected neural network. In section 4, based on a case study of a power community, the feasibility of the proposed IASO-BP model and the Stirling engine-based microgrids is analysed. Finally, the main conclusions are drawn in section 5.

1. SECOND-ORDER ADIABATIC MODEL

1.1 Mathematical Models

In second-order analysis, the structure of the Stirling engine is simplified. It only consists of the expansion chamber (e), the heater (h), the cooler (k), the regenerator (r) and the compression chamber(c). The simplified configuration and temperature curve are displayed as follows.

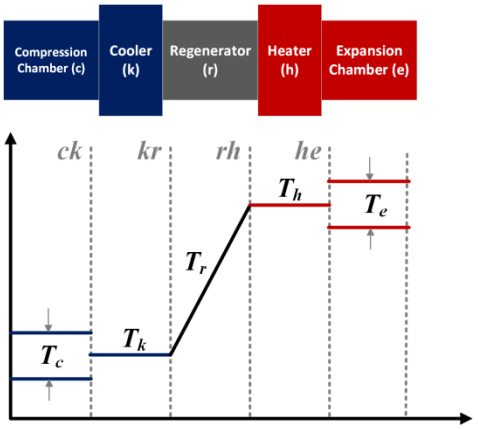

Fig.1. Temperature approximation of second-order analysis

The temperature in the cooler (T_k) and heater (T_h) are constant, while the temperature in the expansion chamber and compression chamber can frequently change during engine operation. The temperature in the regenerator is calculated by the logarithmic mean of T_h and T_k.

$$T_r = \frac{T_h - T_k}{\ln(T_h / T_k)} \tag{1}$$

Besides, the subscripts, *ck*, *kr*, *rh*, *he*, represent the boundary between two constituent elements. In adiabatic analysis, both the compression chamber and expansion chamber are assumed to be adiabatic. Differential governing equations of the early adiabatic model are improved by considering heat transfers of the working fluid to the surrounding in expansion and

compression chambers. The governing equations system is summarised in Table 1.

Table. 1. Governing Equations for Adiabatic Analysis

Parameters	Equations
Mass	
	$m_i = \frac{pV_i}{RT_i} \qquad i = c,k,r,h,e$
	$dm_i = \frac{m_i dp}{p} \qquad i = k,r,h$
	$dm_c = \frac{\left(pdV_c + \frac{V_c}{\gamma}dp\right)}{RT_{ck}} \quad dm_e = \frac{\left(pdV_e + \frac{V_e}{\gamma}dp\right)}{RT_{he}}$
Boundary Mass Flow	
	$m_{ck} = -dm_c \quad m_{kr} = m_{ck} - dm_c$
	$m_{he} = dm_e \quad m_{rh} = m_{he} + dm_h$
Pressure	
	$p = \frac{(m_c + m_k + m_r + m_h + m_e)R}{\left[\frac{V_c}{T_{ck}} + \frac{V_e}{T_{he}} + \gamma\left(\frac{V_k}{T_k} + \frac{V_r}{T_r} + \frac{V_h}{T_h}\right)\right]}$
	$dp = \frac{-\gamma p\left(\frac{dV_c}{T_{ck}} + \frac{dV_e}{T_{he}}\right)}{\left[\frac{V_c}{T_{ck}} + \frac{V_e}{T_{he}} + \gamma\left(\frac{V_k}{T_k} + \frac{V_r}{T_r} + \frac{V_h}{T_h}\right)\right]}$
Temperature	
	$dT_i = T_i\left(\frac{dp}{p} + \frac{dV_i}{V_i} - \frac{dm_i}{m_i}\right) \qquad i = c,e$
	$T_{ck} = \begin{cases} T_c & m_{ck} > 0 \\ T_k & m_{ck} \le 0 \end{cases} \quad T_{he} = \begin{cases} T_h & m_{he} > 0 \\ T_e & m_{he} \le 0 \end{cases}$
Energy	
	$dQ_k = \frac{c_v V_k}{R}dp - c_p(T_{ck}m_k - T_{kr}m_r)$
	$dQ_r = \frac{c_v V_r}{R}dp - c_p(T_{kr}m_r - T_{rh}m_h)$
	$dQ_h = \frac{c_v V_h}{R}dp - c_p(T_{rh}m_h - T_{he}m_e)$
	$dW = pdV_c + pdV_e$

The theoretical power output of the Stirling engine is always higher than the result obtained by experiments. This discrepancy is due to the lack of consideration of the power losses. To bring the simulations in this study closer to the real physical situation, it is required to calculate those losses during the operation.

Heat Loss due to the Displacer Shuttle Conduction

This loss is due to the Shuttle movement of the displacer between the top dead centre (TDC) and the bottom dead centre (BDC) [8]. This kind of loss can be calculated as follows.

$$\begin{cases} \delta Q_{shuttle\_c} = \dfrac{\pi S_c^2 \lambda d_c}{8 x_c L_{pc}}(T_c - T_{ck}) \\ \delta Q_{shuttle\_e} = \dfrac{\pi S_e^2 \lambda d_e}{8 x_e L_{pe}}(T_c - T_{he}) \end{cases} \tag{2}$$

where the subscript *c* and *e* denote the compression chamber and the expansion chamber, *S* represents the stroke of displacer or power piston, *d* represents the internal diameter of the cylinder, *Lp* represents the length of displacer or power piston, x represents the annular gap between the piston and the cylinder, λ represents the gas thermal conductivity.

Polytropic Heat Loss of the Engines Compartment

In the actual operation, the heat transfer between the working fluid and the surrounding through cylinder walls in expansion and compression chambers is inevitable. Therefore, polytropic heat loss is considered.

$$Q_{poly} = mC_v \frac{n-k}{n-1}(T - T_{amb}) \tag{3}$$

where Q_{ploy} represents the polytropic heat loss, T_0 and T are ambient temperature and temperature in the chamber, respectively. The differential form of Q_{poly} is as follows.

$$dQ_{poly} = C_n(T - T_{amb})dm - mC_n dT \tag{4}$$

Heat Loss in Regenerator

To evaluate the regenerator's performance, the parameter called regenerator effectiveness is introduced and can be obtained as follows [10].

$$\begin{cases} \varepsilon = \dfrac{NTU}{1 + NTU} \\ NTU = 0.023\,\mathrm{Re}^{-0.2}\,\mathrm{Pr}^{-0.6}\left(\dfrac{A_{wg}}{A}\right) \end{cases} \tag{5}$$

where *NTU*, A_{wg}, and *A* are the number of the transfer unit and wet and cross-section areas of the regenerator, respectively. *Re* and *Pr* represent Reynolds and Prandtl numbers, respectively. Reynolds number is calculated based on the hydraulic diameter of wire mesh as well as porosity and shape factor of regenerator mesh as mentioned in Ref. [10]. Assuming that the efficiency of the regenerator is equal to ε, then the regenerator inefficiency loss can be calculated as follows.

$$Q_{reg} = Q_r(1 - \varepsilon) \tag{6}$$

where Q_r represents the amount of heat recovery under ideal conditions.

1.2 Results and Discussion

The simplest way of solving the differential equations is to transform this issue into the initial value problem. Because of the periodic nature of the Stirling engine operation, after comparing the initial and final values, the new value for the next iteration can be determined. When the required error between the value of the previous step (y_n) and the value of the current step (y_{n+1}) is accomplished, convergence is obtained.

$$T_{cal\_cycle} = 2\pi \quad T_{step} = \Delta\theta = \frac{2\pi}{360} \tag{7}$$

The Runge-Kutta method is an implicit or explicit iterative approach for solving non-linear ordinary differential equations. Detailed mathematics descriptions of the Runge-Kutta method can be found in the literature [11]. The calculation strategy is displayed in Eq. 10 and Fig.2.

$$\begin{cases} \vec{y} = [T, p, m, W, Q] \\ Y(\theta = n) = Y_n = \overrightarrow{y_n} = [T, p, m, W, Q]_n \\ dY = f(d\theta, dy),\ d\theta = \dfrac{2\pi}{360} \\ Y_{n+1} = Runge - Kutta(Y_n) \end{cases} \tag{8}$$

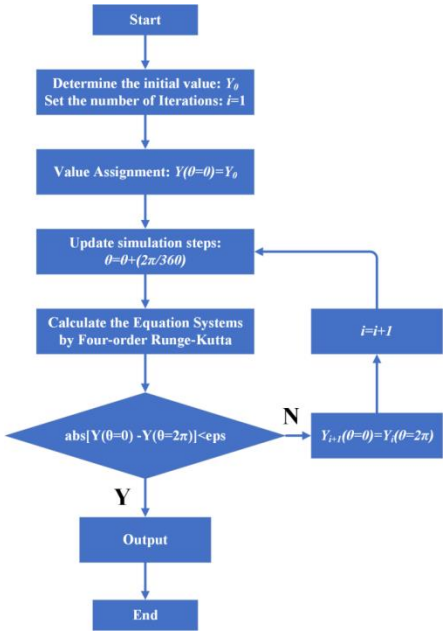

Fig. 2. Calculation Processes of the second-order Stirling engine modelling

The temperatures, pressure and volume of the expansion chamber and compression chamber at the time step $\theta = 2\pi$ can be obtained after one cycle through the Runge-Kutta method. These parameters are then compared with the initially set temperature. Then a judgement is made as to whether the current error is within the accuracy requirements. If convergence is not achieved, the value of *Y* at $\theta = 2\pi$ is specified as the new initial value for the next iteration. The flow chart of the calculation is shown as follows. Table 2 and Figure 3 show the important parameters and chamber motion of the Stirling engine understudy, respectively.

Table 2 Critical Parameters of the Stirling Engine

Parameters	Description or Value
Working Fluid	Hydrogen
Cylinder Number	4
Inside Heater Temperature	649° C
Inlet Cooling Water Temperature	57° C
Engine speed	2000 rpm
Mean Pressure	1400 psia (9653 kPa)
Mechanical Efficiency	0.92
Furnace Efficiency, %	0.85
Cylinder Diameter	72 mm
Piston Stroke	46 mm
Number of Pipes in heater	18
Diameter of Pipes in heater	4.8 mm
Number of Pipes in cooler	156
Diameter of Pipes in cooler	1.2 mm
Efficiency of the Regenerator	0.9

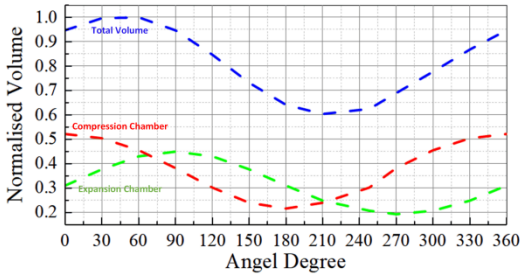

Fig. 3. Volume variation in calculation period

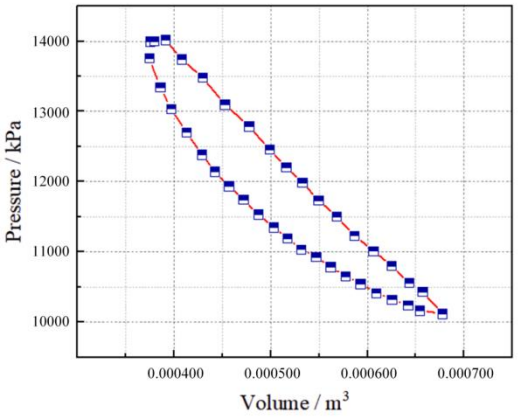

Fig. 4. Pressure-Volume diagram obtained by modified Second-order model

The cyclic mean pressure of the Stirling engine is 10,000 kPa, while the mean pressure of our analytical model is 11,500 kPa. The error is about 15%. This result can be

considered acceptable for a numerical model that contains many idealised assumptions. In the next section, numerical results are used as the training sample to provide guidance and support for the development of machine learning approaches.

2. IMPROVED ATOM SEARCH OPTIMISATION (IASO)

Before building a neural network, a novel method for global search to optimise the network structure is proposed first, called the improved ASO algorithm (IASO). The IASO proposed in this study improves the global search capability and precocity avoidance capability of general ASO through the improvement of strategy. Then, IASO is applied to optimise the weights and thresholds in the neural networks constructed for Stirling engine modelling with multiple parameters. The mathematical expression of the original ASO is in literature [12]. It is an algorithm inspired by molecular dynamics to search and optimise in parameter space by simulating atomic motion. To further improve the searchability and convergence speed of ASO, some improvements are proposed.

Improvement 1: Elite Opposition-based Learning

The Elite opposition-based strategy was proposed by Tizhoosh in 2005 [14] and has been successfully applied in several intelligence optimisation algorithms such as GA, PSO, and ACO. The mathematical expression of inverse solution (p^*) of p is as follows.

$$\begin{aligned} &p=(x_1,x_2,...,x_D),\ x_i\in[l_i,u_i],\ p\in R^D \\ &p^*=(x^*_1,x^*_2,...,x^*_D),\ x^*_i=l_i+u_i-x,\ p^*\in R^D \end{aligned} \tag{9}$$

The introduction of the inverse solution allows the search area of the algorithm to be extended. Assuming that $x_i(t)=(x_{i1},x_{i2},...,x_{iD})$ is a solution set in *i-th* iteration and $f(x)$ represents the object function. The elite individuals ($N_i(t)$) and ordinary individuals ($Q_i(t)$) for the *N-th* iteration are defined as follows.

$$\begin{cases} x_i(t)\in N_i(t),\ f(x_i(t))<f(x_i(t)^*) \\ x_i(t)\in Q_i(t),\ f(x_i(t))\geq f(x_i(t)^*) \end{cases} \tag{10}$$

The elite opposite solution can be calculated as follows.

$$x^*_{ij}(t)=k\cdot[a_j(t)+b_j(t)]-x_{ij}(t),k\in rand[0,1] \tag{11}$$

where, x_{ij} represents the value of *i-th* individual in dimension *j;* k is a random number. The interval constructed by the elite population $[a_j(t),\ b_j(t)]$ is as follows.

$$\begin{aligned} a_j(t)&=\min[N_{1j}(t),...,N_{pj}(t)] \\ b_j(t)&=\max[N_{1j}(t),...,N_{pj}(t)] \end{aligned} \tag{12}$$

Improvement 2: Inertia Weight

To improve the convergence speed of the algorithm, an inertia weight is introduced, which is defined as follows.

$$w=2\cdot\left(1-\frac{t}{MaxIter}\right) \tag{13}$$

where, *t* represents the current number of iterations and *MaxIter* represents the maximum number of iterations. The inertia factor is introduced into the position update equation for the atom, as is shown.

$$X(t+1)=wX(t)+v(t) \tag{14}$$

Improvement 3: Dimensional Gaussian Mutation

To improve the global search capability, a gradual Gaussian variation is used for variation for the optimal position, and then a greedy strategy is used to retain the most optimal solution.

$$\begin{aligned} X_{bestnew}(j)&=X_{best}(j)+randn\times X_{best}(j) \\ X_{best}&=\begin{cases} X_{bestnew},\ f(X_{bestnew})<f(X_{best}) \\ X_{best},\ f(X_{bestnew})\geq f(X_{best}) \end{cases} \end{aligned} \tag{15}$$

To fully demonstrate the superiority of IASO, 23 testbench functions for testing algorithms in literature [13] are used in the experiments. Those testbench functions can be divided into three categories, namely the unimodal function, the multimodal function and the fixed-dimension function. IASO has shown a considerable performance improvement in 23 typical test functions. Typical results of the unimodal, multimodal, and fixed-dimension function are shown in Fig. 5(a), Fig. 5(b), and Fig. 5(c), respectively.

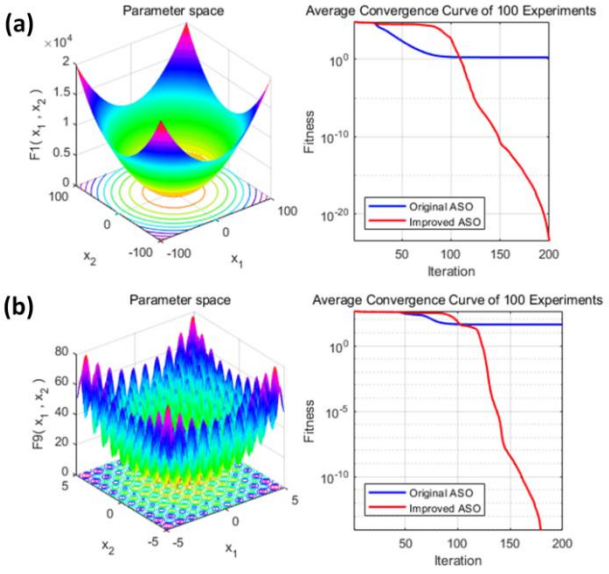

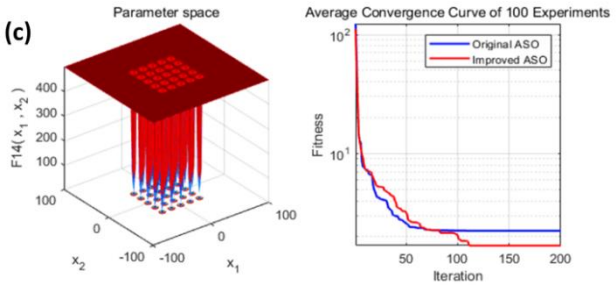

Fig. 5. Performance of Convergence Speed and Search Ability in Unimodal, Multimodal and Fixed-dimension Functions

3. DEEP LEARNING SOLUTION: IASO-BP

The IASO integrated BP neural network model named IASO-BP for Stirling engine operation modelling is proposed in this section. The schematic diagram of the IASO-BP is displayed as follows.

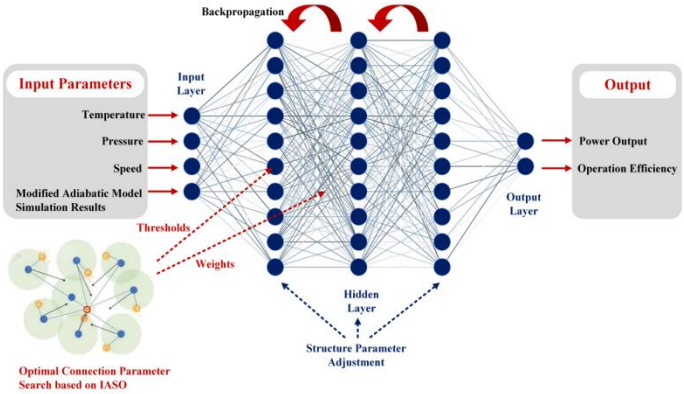

Fig. 6. Algorithm schematic of ISAO-BP Stirling Engine Output and Efficiency Model

The output layer contains two neurons that has able to export the power and efficiency signals synchronously. The IASO-BP model is applied to establish the mapping between 280 sets of operation parameters (temperature, pressure, speed, and power obtained by second-order adiabatic analysis in section 1), and 280 sets of experimental data including power output and operation efficiency.

The regression performance of the IASO-BP model for training, validation and testing is shown in Figure 7. To enhance the persuasiveness of the results, data that never appeared in the training sample, representing 25% of the total sample, are selected as the test set. Results of test set are displayed in Figure 8. After sufficient training, the IASO-BP model can export the cycle power and efficiency simultaneously and achieve 95% calculation accuracy. Moreover, the spatial surfaces of power - operation conditions and efficiency - operation conditions are constructed in Fig. 9.

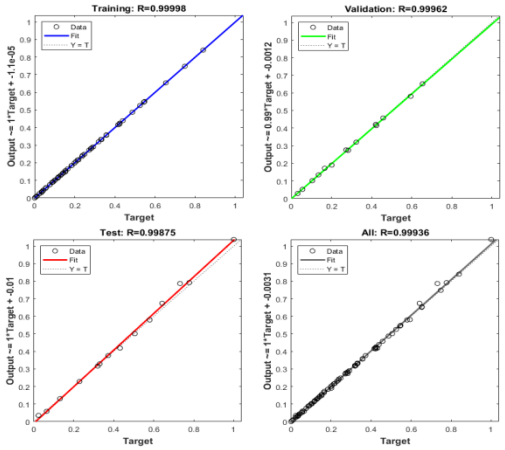

Fig. 7. Regression Performance of the IASO-BP model

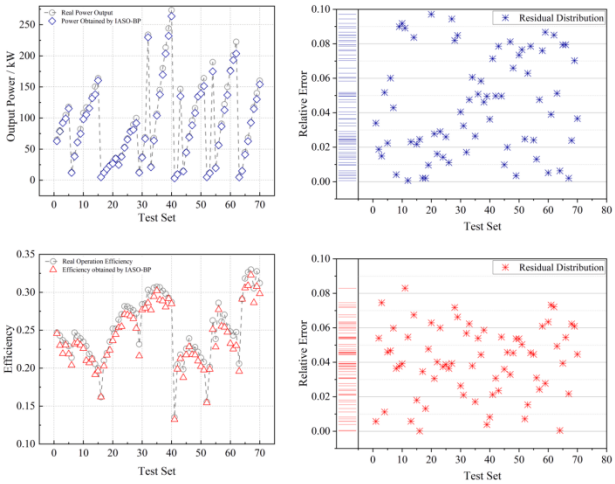

Fig. 8. Results of power and efficiency modelling

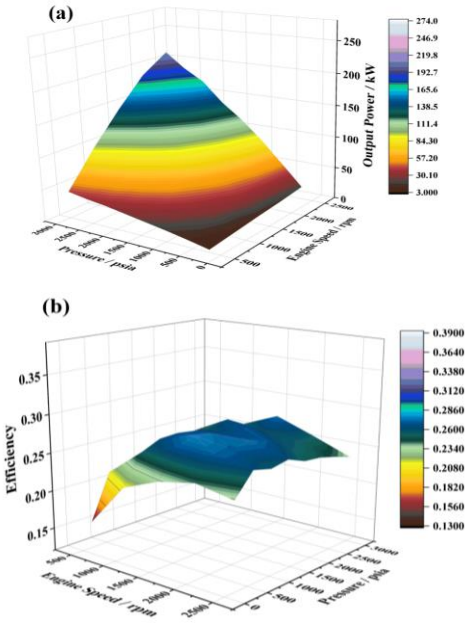

Fig. 9. Curved surface of cycle power and operation efficiency constructed by IASO-BP

Figure 9 indicates that the efficiency is more sensitive to changes in operating conditions, containing areas of stable efficiency and also areas of sudden increase. With a given power, the difference in efficiency can be significant depending on the operating conditions. The 'efficiency surfaces' obtained by IASO-BP encompass a wide range of possible scenarios and has certain engineering application significance. The data points on these surfaces are 95% similar to the real experimental results, which is a huge improvement compared to the accuracy of 80% in second-order adiabatic analysis. The IASO-BP model has successfully learned the mapping relationship between the numerical model and experimental solutions.

4. CASE STUDY

After obtaining the accurate output model, a Stirling engine - Photovoltaic microgrid using supercomputer waste heat recovery is constructed in figure 10. This energy community is in the suburban area of London and mainly consists of Stirling engines array, generators, PV panels, and storage units. Figure 12 and figure 13 display the annual solar radiation intensity and waste heat source temperature profiles separately.

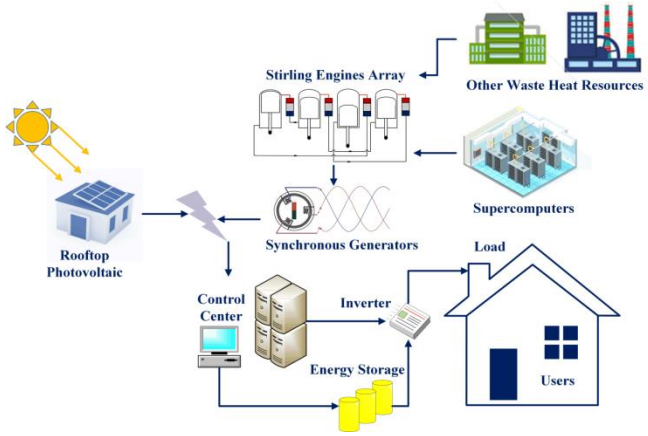

Fig. 10. Stirling engine -PV integrated microgrid

The objective function for system optimisation is energy losses and energy volatility. The indicator of energy losses (I_{losses}) refers to the surplus generation after meeting user demands and energy storage, while the indicator of energy volatility ($I_{volatility}$) refers to the proximity between generation and demands. The constraints are mainly in terms of installed capacity and the average annual efficiency of engines. The objective functions are described by Equation 16 and Equation 17 while constraints can be calculated by Equation 18 and Equation 19.

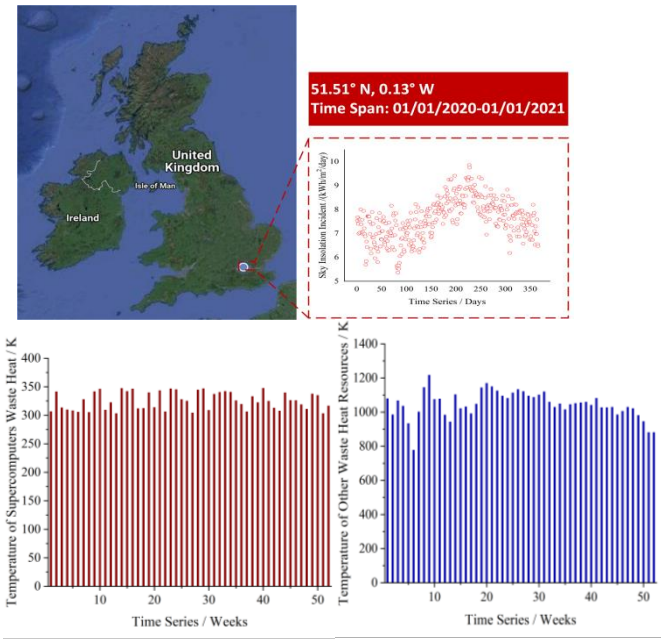

Fig. 11. Annual sky insolation incident and Temperature profile of waste heat resources

Figure 12 shows the composition and process of the optimisation. Furthermore, Figure 13 displays the optimum annual operation plan for the Stirling engine, PV panels and Storage units after configuration optimisation. Profound energy complementarity between generations and loads is finally obtained.

$$P_{Gen}(t) = P_{SE}(t) + P_{PV}(t) + P_{Bat}(t-1)$$

$$I_{Losses} = \frac{P_{Gen}(t) - P_{Load}}{P_{SE}(t) + P_{PV}(t)} \quad (16)$$

$$I_{Volatility} = \sqrt{\frac{1}{n}\sum_{i}^{n}\left\{P_{Gen}(t) - \left[P_{Bat}(t) + P_{Load}(t)\right]\right\}^2} \quad (17)$$

$$\bar{\eta}_{ST} = \frac{1}{n}\sum_{i=1}^{n}\eta_i \geq \eta_{reliability} \quad (18)$$

$$0 \leq N_{ST} \leq N_{ST\_Max} \quad 0 \leq N_{PV} \leq N_{PV\_Max} \quad (19)$$

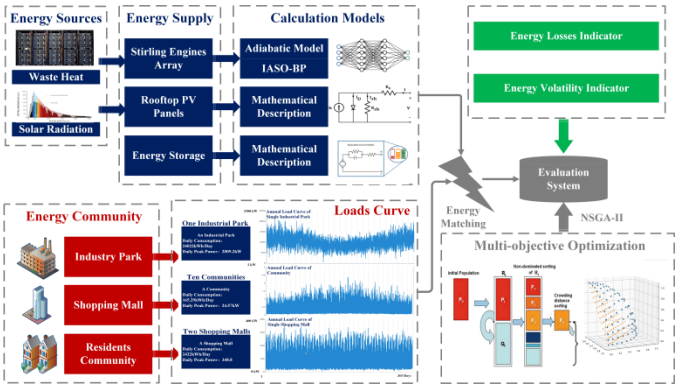

Fig. 12. Schematic diagram of optimisation implementation

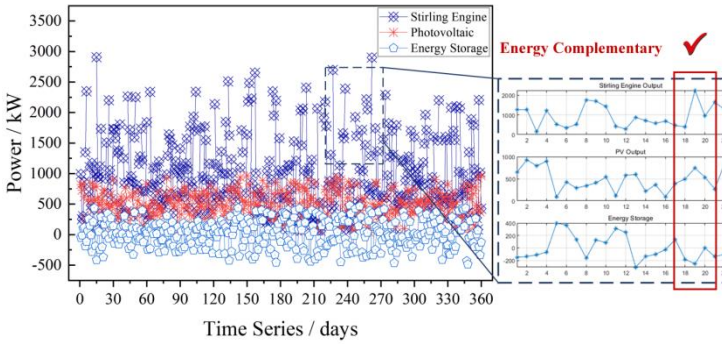

Fig. 13 Results on annual generation scheduling

5. CONCLUSION

In this study, a modified second-order adiabatic model is conducted. To further improve the accuracy and investigate both power output and efficiency, an IASO-BP model adapted to the Stirling engine analysis problem is proposed. The main research findings are as follows:

(1) The modified second-order model contains a considerable amount of thermodynamic information and is a sufficient guide to establish the mapping to accurate experimental results.

(2) The IASO approach improved by elite opposition-based learning and dimensional Gaussian mutation has significantly enhanced both convergence speed and global search ability. Results obtained by IASO-BP can achieve a prediction accuracy of 95% in terms of simultaneous prediction of power output and efficiency.

(3) A regional microgrid containing Stirling engines for waste heat recovery is developed. Based on the proposed model and multi-objective, profound energy complementary is achieved, guiding the industrial application of Stirling engines.

ACKNOWLEDGEMENT

Support from the UK Engineering and Physical Sciences Research Council (EPSRC) under the project “Exascale Computing for System-Level Engineering: Design, Optimisation and Resilience” (Grant No. EP/V001531/1) is gratefully acknowledged.

REFERENCE

[1] Erol D, Yaman H, and Doğan B. A review development of rhombic drive mechanism used in the Stirling engines. Renew Sust Energ Rev 2017; 78:1044-1067.

[2] Yang HS, Cheng CH. Development of a beta-type Stirling engine with rhombic-drive mechanism using a modified non-ideal adiabatic model. Appl Energ 2017;200:62-72.

[3] Cheng CH, Yu YJ. Numerical model for predicting thermodynamic cycle and thermal efficiency of a beta-type Stirling engine with rhombic-drive mechanism. Renew Energ 2010;35(11):2590-2601.

[4] Timoumi Y, Tlili I, Ben Nasrallah S. Design and performance optimisation of GPU-3 Stirling engines. Energy 2008;33(7):1100–1114.

[5]Ni M, Shi B, Xiao G, Peng H, Sultan U, Wang S, Luo Z, Cen K. Improved Simple Analytical Model and experimental study of a 100 W β -type Stirling engine. Appl Energ 2016;169:768-787.

[6] Li R, Grosu L, Queiros-Condé D. Losses effect on the performance of a Gamma type Stirling engine. Energ Convers Manage 2016;114:28-37.

[7] Li R, Grosu L, Li W. New polytropic model to predict the performance of beta and gamma type Stirling engine. Energy 2017;128:62-76.

[8] Hachem H, Gheith R, Aloui F, Ben Nasrallah S. Numerical characterisation of a γ -Stirling engine considering losses and interaction between functioning parameters. Energ Convers Manage 2015;96:532-543.

[9] Babaelahi M, Sayyaadi H. A new thermal model based on polytropic numerical simulation of Stirling engines. Appl Energ 2015;141:143-159.

[10] Babaelahi M, Sayyaadi H. Modified PSVL: A second order model for thermal simulation of Stirling engines based on convective-polytropic heat transfer of working spaces. Appl Therm Eng 2015;85:340-355.

[11] Rothe S, Hamkar AW, Quint KJ, Hartmann S. Comparison of diagonal-implicit, linear-implicit and half-explicit Runge-Kutta methods in non-linear finite element analyses. Arch Appl Mech 2012;82(8):1057-1074.

[12] Zhao W, Wang L, Zhang Z. Atom search optimisation and its application to solve a hydrogeologic parameter estimation problem. Knowl-based Syst 2019;163:283-304.

[13] Khalilpourazari S, Khalilpourazary S. An efficient hybrid algorithm based on Water Cycle and Moth-Flame Optimization algorithms for solving numerical and constrained engineering optimisation problems. Soft Comput 2017;23(5):1699-1722.